

N87-15345

D/6-32

R/b

TDA Progress Report 42-87

July - September 1986

# A New Algorithm for Microwave Delay Estimation From Water Vapor Radiometer Data

S. E. Robinson

Tracking Systems and Applications Section

*A new algorithm has been developed for the estimation of tropospheric microwave path delays from water vapor radiometer (WVR) data, which does not require site and weather dependent empirical parameters to produce high accuracy. Instead of taking the conventional linear approach, the new algorithm first uses the observables with an emission model to determine an approximate form of the vertical water vapor distribution which is then explicitly integrated to estimate wet path delays, in a second step. The intrinsic accuracy of this algorithm has been examined for two channel WVR data using path delays and simulated observables computed from archived radiosonde data. It is found that annual RMS errors for a wide range of sites are in the range from 1.3 mm to 2.3 mm, in the absence of clouds. This is comparable to the best overall accuracy obtainable from conventional linear algorithms, which must be tailored to site and weather conditions using large radiosonde data bases. The accuracy and flexibility of the new algorithm are indications that it may be a good candidate for almost all WVR data interpretation.*

## I. Introduction

Very Long Baseline Interferometry (VLBI) and Global Positioning System (GPS) applications, as well as other fields, require calibration of microwave delays caused by water vapor in the troposphere. Two and three channel water vapor radiometers (WVRs) are increasingly seen as the best solution to this problem. Unfortunately, WVRs do not directly measure delay; they actually measure antenna temperatures in frequency channels close to the 22.2 GHz resonance of water. The WVR observables must then be related to the desired wet path delays by a data interpretation algorithm. In order to

most effectively use the WVR data, one must, therefore, understand and quantify the level of error in the delay estimation contributed by the algorithm itself.

The most popular algorithm formulation, resulting from the conventional approach to delay estimation, assumes that the microwave delay may be written as a linear expansion in the total optical depths of the troposphere at the WVR channel frequencies (e.g., Refs. 1, 3, and 6). The optical depth at any point  $s$ , for a frequency  $\nu$ , is defined by the integral along the line-of-sight in the atmosphere,

$$\tau(s, \nu_i) = \int_0^s ds' \alpha(s', \nu_i)$$

The total optical depth to be used in the delay expansion is, therefore, just  $\tau(\infty, \nu_i)$ . The symbol  $\alpha$  represents the extinction coefficient, also called opacity (e.g., Ref. 5, page 23), a complicated function of temperature, pressure, frequency, and the densities of water vapor and liquid, that is defined by an atmospheric emission model (e.g., Refs. 9 and 10). In the linear algorithms, the  $\tau(\infty, \nu_i)$  are usually estimated from the antenna temperatures after assuming effective radiating temperatures for the tropospheric water vapor. The coefficients in the linear delay expansion, sometimes called retrieval coefficients (see Ref. 3), are determined empirically, usually using a set of wet delays and corresponding simulated WVR antenna temperatures computed from archived radiosonde data. Once the delay coefficients have been determined by regression analysis of the simulated observables, the WVR user has a very simple, easily applied, expression for wet delay.

There are also undesirable features of linear delay algorithms, as with most other algorithms. In particular, the linear coefficients must be empirically tailored to each observing site and set of observing conditions in a process sometimes called stratification, in order to achieve high delay estimation accuracy (Ref. 3). The need for this arises from the fact that the WVR antenna temperatures and surface meteorology data do not uniquely define the implicit parameters of the delay estimation problem. Specifically, the WVR antenna temperatures,  $T_a(\nu_i)$ , are imperfect measurements of the radiation brightness temperatures, which are given by

$$T_b(\nu_i) = \int_0^{\tau(\infty, \nu_i)} d\tau T_k(\tau) \exp(-\tau) + T_{bg} \exp(-\tau(\infty, \nu_i))$$

or, equivalently,

$$T_b(\nu_i) = \int_0^{\infty} ds \alpha(s, \nu_i) T_k(s) \exp(-\tau(s, \nu_i)) + T_{bg} \exp(-\tau(\infty, \nu_i))$$

where  $\tau$  is defined above,  $T_k$  is the kinetic temperature, and  $T_{bg}$  is the background temperature. Because of the dependence on  $\tau$  and  $\alpha$ , the WVR observables also depend on the distributions of temperature, pressure, and water liquid, as well as the actual amount of water vapor along the line-of-sight. The conventionally defined wet path delay has a simpler form,

$$R_{\text{wet}} \propto \int_0^{\infty} ds \rho_v(s)/T_k(s)$$

but also depends on the distribution of water vapor density,  $\rho_v(s)$ , and the temperature profile (e.g., Ref. 2). One can see from these expressions that only a knowledge of the line-of-sight temperature, pressure, water vapor, and water liquid distributions can uniquely specify both brightness temperatures and wet path delay. Since this information is not directly available in observable quantities, the past values of the required data under specific conditions are used to improve the definitions of the linear delay coefficients.

Stratification of the coefficients requires that a large radiosonde data base be available for the empirical estimation of each coefficient set. The first difficulty that this presents is that of simply matching coefficients to individual sites. Since radiosondes are flown at relatively few locations which are usually near population centers and away from most radio observatories, there is nearly always some uncertainty in the association of a data base with any specific site of interest. In addition, even with the currently discussed computation of delay coefficients for specific seasons, weather conditions, and sites, use of the linear algorithm may become awkward when processing typical VLBI and GPS experiments. Finally, the delay estimation accuracy of the linear algorithms cannot be improved indefinitely by simply increasing the level of stratification, because of the finite number of meaningful observable criteria for discrimination.

In order to avoid the disadvantages of linear algorithms, a new algorithm, the profile algorithm, has been developed from an entirely different approach. The new algorithm's formulation of the delay estimation problem relies on the direct application of the known physics of the problem to make better use of observables, rather than on large data bases to adjust linear delay coefficients for specific conditions. The result is more complex than the linear algorithms, but has considerable advantages. Most notably, it offers complete independence from site and condition-specific empirical parameters, and their inherent problems, while producing delay estimation accuracy that is as good as that of the better stratified linear algorithms.

## II. Description of the Profile Algorithm

The basic premise of the profile algorithm is that an actual solution to a simplified version of the nonlinear delay problem can be generated numerically from each WVR observation and the corresponding surface meteorology. This leads to a formulation and an execution very unlike those for the linear algorithms. In fact, the profile algorithm makes no attempt to impose a direct relationship, linear or otherwise, between WVR antenna temperatures and wet path delays. Instead, simple vertical distributions of water vapor and liquid are

adjusted until they produce, through an atmospheric emission model (e.g., Ref. 10), brightness temperatures in agreement with the WVR antenna temperatures. The delay estimates themselves are produced in a second step by integrating along the line-of-sight using the fitted water vapor distributions.

It is assumed that the vertical distribution of the relative humidity can be adequately represented by a two piece linear function. At surface level, the relative humidity is naturally given by surface meteorology, and at altitude of 10 km, so little water vapor can exist that it can safely be taken as zero. The relative humidity profile is then approximated by connecting the two end points linearly to the relative humidity at an intermediate altitude of 3 km. It is the value of the relative humidity at this point that the algorithm freely adjusts in order to completely specify the vapor profile. An example of such a simplified water vapor profile used by the profile algorithm is illustrated on the left side of Fig. 1. The corresponding water vapor density profile, defined by the sample relative humidity distribution, is shown in the right portion of the figure.

The vertical pressure and temperature profiles must also be known, or assumed, in order to specify the water vapor density and opacity from the algorithm's relative humidity profile. The pressure can be well represented by an exponential decay from the surface value. The temperature profile for the profile algorithm is produced by first creating a nominal temperature profile from data in Tables 5.1 and 5.2 of the Standard Atmosphere (Ref. 12), interpolated to the latitude and altitude of the site, and to the time of year of the observation. The surface temperature implied by the nominal profile is then subtracted from the measured surface temperature and multiplied by  $\exp(-h/H)$ , where  $h$  is the altitude, and  $H$  is a constant scale height, to produce an altitude-dependent temperature correction. The temperature profile used by the algorithm is then formed by adding the nominal profile and the correction. It, therefore, matches the measured surface temperature, and exponentially approaches the nominal temperature distribution as the altitude increases. An examination of temperature profiles from radiosondes at a number of locations suggests that the best choice of scale height for the decay of the surface temperature adjustment is about 2 km. An example of such an adjusted profile is shown in Fig. 2. Note that the site altitude and latitude, needed to produce the nominal temperature profiles, are the only site-specific parameters required by the profile algorithm.

In reality, the actual vertical water vapor distributions deviate from the assumed form of the profiles; however, the impact of these differences is quite small, as the next section of this article demonstrates. One reason for this is that the channel frequencies of the WVRs are usually selected so as to

minimize the influence of changes in the vertical water vapor profiles on estimated delay (Refs. 7 and 11). Another is that in integrating the vapor distribution to find the wet delay, high frequency spatial variations tend to average out, making a smooth function an adequate representation. Still, dependence on the vertical structure cannot be completely eliminated, so the fact that the new algorithm provides even an approximate adjustment to the effective height of the water vapor gives some improvement over the linear algorithms.

In the simulations that are described in the next section, it is assumed that the liquid opacity is negligible, but in actual use the delay estimation algorithm must accurately account for the continuum emission from water droplets in clouds in order to produce high quality delay estimates. The liquid opacity is not a function of pressure, and only weakly dependent on temperature (e.g., Ref. 9), which means that the liquid contribution to the WVR antenna temperatures is relatively insensitive to the actual form of the vertical distribution of droplets. Therefore, the simple assumption that the water liquid density is proportional to the saturation water vapor density at any point has been made, and the algorithm is allowed to fit for the constant of proportionality. The effect of this assumption will be examined in work, unfinished at the time of this writing, dealing with algorithm performance in the presence of clouds.

### III. Accuracy of the Profile Algorithm

All algorithms for the estimation of wet path delays from WVR data contribute some error to the final estimates. This error is intrinsic to the algorithm, and as such can be separated from other error sources. The best way to isolate and quantify the algorithm error is by generating simulated WVR antenna temperatures and corresponding wet path delays from a set of vertical profiles of water density, temperature, and pressure. This is a process similar to that used to generate empirical coefficients for linear algorithms, as described by Gary et al. (Ref. 3), Resch (Ref. 6), and others. Such a simulation has been done for the new profile algorithm, and the results are described in this section.

Radiosonde data are taken on a regular basis at a large number of sites over the world, and can be used as the basis of the required simulation. These data typically consist of temperature and relative humidity on a vertical grid of pressure, which can be converted to altitude. For our simulation, data were obtained spanning a full year for 16 sites of interest. Some sites were selected from the available radiosonde archive because they were closest to prominent VLBI observatories, others were chosen to overlap with other delay retrieval accuracy studies, and the rest were picked to produce a good cross-section of locations in the continental United States.

Although 13 of the data sets contained two radiosonde profiles for most days, Edwards AFB, Madrid, and Wagga-Wagga had less than half that number available. These were, nonetheless, included because of their proximity to Goldstone, DSS 63, and DSS 43, respectively. Radiosonde profiles which had missing or blatantly erroneous data below 5 km, or which terminated at anomalously low altitudes, were removed by software to avoid corruption of the results. This left an average of 645 profiles for all but the three previously mentioned sites, which averaged 260. Examination of the rejected data revealed no selection effects that could bias the simulation.

Next, each profile was used to compute a zenith delay, due to water vapor, and the corresponding antenna temperatures that would be observed by an ideal noise-free WVR with frequency channels at 20.7 GHz and 31.4 GHz. This particular WVR configuration was selected because it corresponds to the majority of existing water vapor radiometers. The emission model used to calculate the WVR observables is essentially that of Waters (Ref. 10) with oxygen opacities given by Rozenkranz (Ref. 8). Because the same emission model was used for both the simulation and the delay retrieval, all emission model errors should cancel in the simulation. Of course, these errors will contribute to the ultimate delay estimation accuracy, but they are the same for all algorithms. No cloud contribution to the continuum emission was used, at this time, because no information concerning liquid content is present in the radiosonde profiles, and a suitable cloud model had not yet been implemented.

Finally, the simulated WVR antenna temperatures and surface meteorology data were used as input to the profile algorithm to produce the delay estimates. The level of algorithm error is then given by the difference between the retrieved delay estimates and the corresponding delays computed directly from the radiosonde profiles. These results for all 16 sites appear in Table 1. The last column displays the root-mean-square algorithm error for the entire year at each location. These range from 1.3 mm for Wagga-Wagga up to 2.3 mm for Munich, and have an average value of 1.8 mm. The annual average zenith delay and the maximum error in estimated delay are also displayed in the table.

Resch presented several variations on the linear delay retrieval algorithm in his 1983 paper (Ref. 6). The most popular, and most accurate, makes use of surface meteorology, and fits the standard form of the linear algorithm given below.

$$R_{\text{wet}} = c_0/\mu + a_0 + a_1 \tau(\infty, \nu_1) + a_2 \tau(\infty, \nu_2)$$

$R_{\text{wet}}$  is the wet path delay estimate, the  $a_i$  and  $c_0$  are empirically determined constants, and  $\mu$  is the cosine of the zenith

angle of the observation. The  $\tau(\infty, \nu_i)$  are optical depth estimates, corresponding to the WVR frequency channels, computed from

$$\tau(\infty, \nu_i) = -\ln [(T_{\text{eff}}(\nu_i) - T_a(\nu_i))/(T_{\text{eff}}(\nu_i) - 2.9)]$$

The  $T_{\text{eff}}(\nu_i)$  in the above equation are empirically determined effective radiating temperatures, computed by fitting to simulated WVR observations, and the  $T_a(\nu_i)$  are the measured antenna temperatures.

For this algorithm, Resch determined best-fits to site-specific linear delay coefficients using 90 radiosonde profiles to cover a one-year period for each of five different locations. He then presented the root-mean-square errors of those fits to the data bases under the same assumptions of no liquid opacity and no WVR noise that were used in the simulations here. The results in this article may, therefore, be compared directly to his for these five sites, as has been done in Table 2. Although the errors for the individual sites are generally different, the average RMS error, at 2 mm, is not significantly different for the stratified linear algorithm and the profile algorithm with no empirically determined site-specific parameters, at all.

#### IV. Discussion and Conclusions

Because of its need to perform emission model calculations, the profile algorithm is required to do a relatively large amount of computation in order to estimate delays from WVR observations. Linear algorithms, on the other hand, require extensive calculations to initially produce linear delay coefficients, but thereafter need very little computation to produce delay estimates. This is not a serious drawback for the new algorithm, however, since even the microcomputers that run the more recent WVRs, such as Janssen's J01 (Ref. 4), are fully capable of running real-time software implementing the profile algorithm. The emission model calculations also produce a definite advantage in that the tropospheric emission characteristics are imperfectly known, and subject to revision. Any emission model changes made to the profile algorithm code can immediately be used for reducing data without delay. In contrast, linear algorithms require a repetition of the lengthy simulations, reprocessing all of the radiosonde data originally used to generate the linear delay coefficients, before new delay estimates may be produced.

There may well be instances when WVR users would prefer to spend only the smaller amount of computation time needed by the linear algorithms, without accepting their less desirable features. For such situations, suitable hybrid schemes can be devised. For example, the profile algorithm is particularly well-suited for use with tipping-curve reduction programs; a

very simple extension would allow it to use the tipping-curve data to simultaneously produce linear delay coefficients, which could then be used for delay estimation until the next invocation of the profile algorithm. There are, of course, many other possible ways of making the best use of both types of algorithms in combination.

The work presented here demonstrates the validity of the profile algorithm and, since many other related formulations are possible, the approach to the WVR delay estimation problem that the new algorithm represents. The most serious question still to be addressed is the profile algorithm accuracy

in the presence of clouds. Preliminary indications from work now in progress are that, while cloudy weather does decrease the delay estimation accuracy, the overall algorithm accuracy is not degraded by more than 15 percent by the addition of liquid opacity to the simulations. Even without the liquid opacity information, the flexibility of the new algorithm, and its apparent ability to use the same procedures and parameters to reduce WVR data from any site under a wide range of weather conditions, while still obtaining high delay estimation accuracy, may make it a good candidate for use with almost all WVR applications. Additional work to thoroughly investigate its properties is certainly justified.

## Acknowledgment

We would like to thank Don Trask for his helpful discussions and encouragement in developing this algorithm.

## References

1. Claflin, E. S., Wu, S. C., and Resch, G. M., "Microwave Radiometer Measurement of Water Vapor Path Delay: Data Reduction Techniques," *DSN Progress Report 42-48*, pp. 22-30, Jet Propulsion Laboratory, Pasadena, CA, Dec. 15, 1978.
2. Crane, R. K., "Refraction Effects in the Neutral Atmosphere," *Methods of Experimental Physics: Astrophysics*, M. L. Meeks, ed., Vol. 12, Part B, pp. 186-200, 1976.
3. Gary, B. L., Keihm, S. J., and Janssen, M. A., "Optimum Strategies and Performance for the Remote Sensing of Path-delay Using Ground-based Microwave Radiometers," *IEEE Transactions on Geoscience and Remote Sensing*, Vol. GE-23, No. 4, pp. 479-484, July 1985.
4. Janssen, M. A., "A New Instrument for the Determination of Radio Path Delay Due to Atmospheric Water Vapor," *IEEE Transactions on Geoscience and Remote Sensing*, Vol. GE-23, No. 4, pp. 485-490, July 1985.
5. Mihalas, D., *Stellar Atmospheres*, W. H. Freeman and Company, San Francisco, CA, p. 23, 1978.
6. Resch, G. M., "Inversion Algorithms for Water Vapor Radiometers Operating at 20.7 and 31.4 GHz," *DSN Progress Report 42-76*, pp. 12-26, Jet Propulsion Laboratory, Pasadena, CA, Feb. 15, 1984.
7. Resch, G. M., "Another Look at Optimum Frequencies for a Water Vapor Radiometer," *DSN Progress Report 42-76*, pp. 1-11, Jet Propulsion Laboratory, Pasadena, CA, Feb. 15, 1984.

8. Rosenkranz, P. W., "Shape of the 5 mm Oxygen Band in the Atmosphere," *IEEE Transactions on Antennas and Propagation*, Vol. AP-23, No. 4, pp. 498-506, July 1975.
9. Staelin, D. H., "Measurements and Interpretations of the Microwave Spectrum of the Terrestrial Atmosphere near 1-cm Wavelength," *Journal of Geophysical Research*, Vol. 71, pp. 2875-2882, 1966.
10. Waters, J. W., "Absorption and Emission by Atmospheric Gases," *Methods of Experimental Physics: Astrophysics*, M. L. Meeks, ed., Vol. 12, Part B, pp. 142-175, 1976.
11. Wu, S. C., "Optimum Frequencies of a Passive Microwave Radiometer for Tropospheric Path-Length Correction," *IEEE Transactions on Antennas and Propagation*, Vol. AP-27, No. 2, pp. 233-239, Mar. 1979.
12. *U. S. Standard Atmosphere Supplements, 1966*, Tables 5.1-5.2, pp. 99-203, prepared under sponsorship of ESSA, NASA, and the USAF, U. S. Government Printing Office, Washington, DC, 1966.

**Table 1. Profile algorithm errors for 1979**

Site	Average delay, cm	Maximum error, cm	RMS error, cm
Albuquerque	7.4	0.55	0.17
Apalachicola	18.0	0.85	0.19
Boise	7.4	0.52	0.16
Dayton	12.3	0.90	0.20
Denver	6.6	0.62	0.14
Edwards AFB	6.6	0.51	0.17
El Paso	8.7	0.92	0.17
Goteborg	8.0	0.77	0.16
Madrid	10.4	0.95	0.19
Munchen	10.0	0.81	0.23
Oakland	9.0	0.64	0.20
Oklahoma City	12.5	0.93	0.20
Pittsburgh	11.0	0.77	0.18
Portland (ME)	10.3	0.97	0.22
San Diego	9.0	0.84	0.22
Wagga-Wagga	9.1	0.41	0.13
		Minimum RMS error	0.13
		Maximum RMS error	0.23
		Average RMS error	0.18

**Table 2. Comparison of errors from profile and Resch algorithms**

Site	Average delay, cm	Profile RMS error, cm	Resch RMS error, cm
El Paso	8.7	0.17	0.14
Oakland	9.0	0.20	0.27
Pittsburgh	11.0	0.18	0.16
Portland (ME)	10.3	0.22	0.18
San Diego	9.0	0.22	0.30
		Minimum RMS error	0.14
		Maximum RMS error	0.30
		Average RMS error	0.21

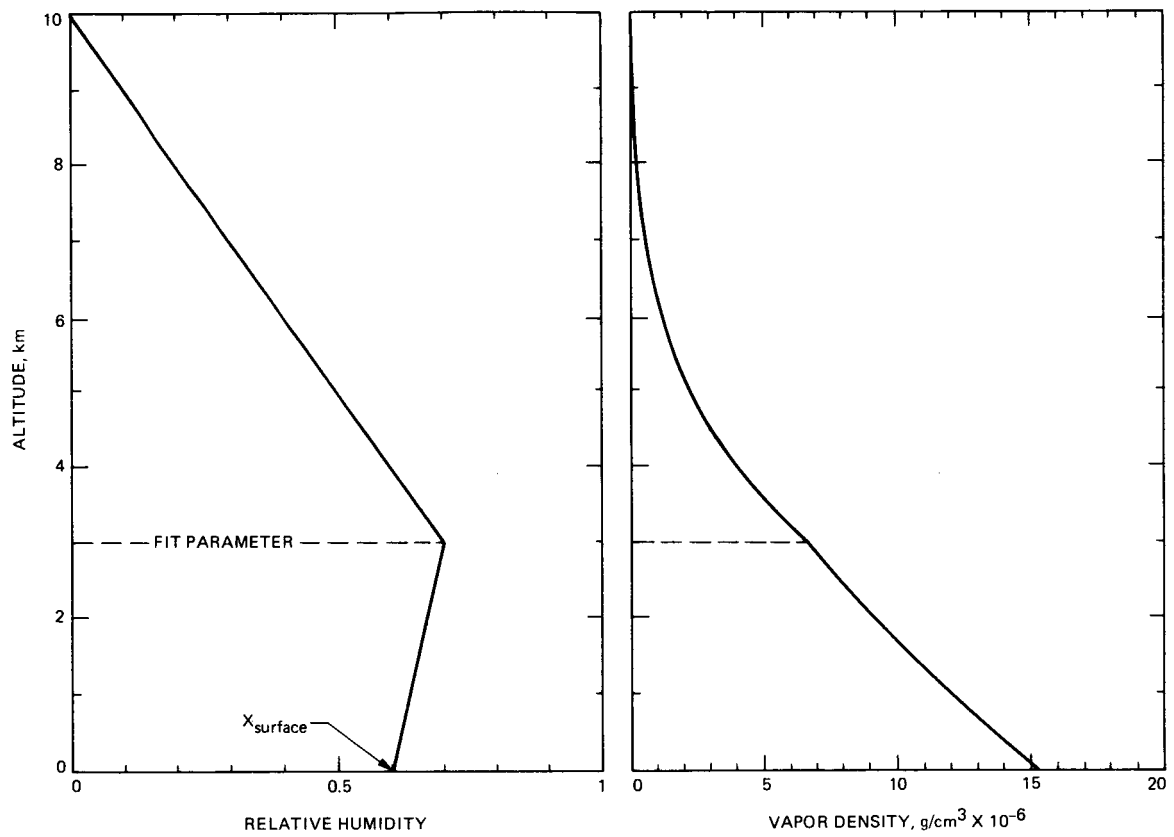


**Fig. 1.** An example of the assumed relative humidity profile appears on the left. The dashed line at 3 km represents the value of the fitting parameter. The water vapor density profile corresponding to the relative humidity is shown on the right.



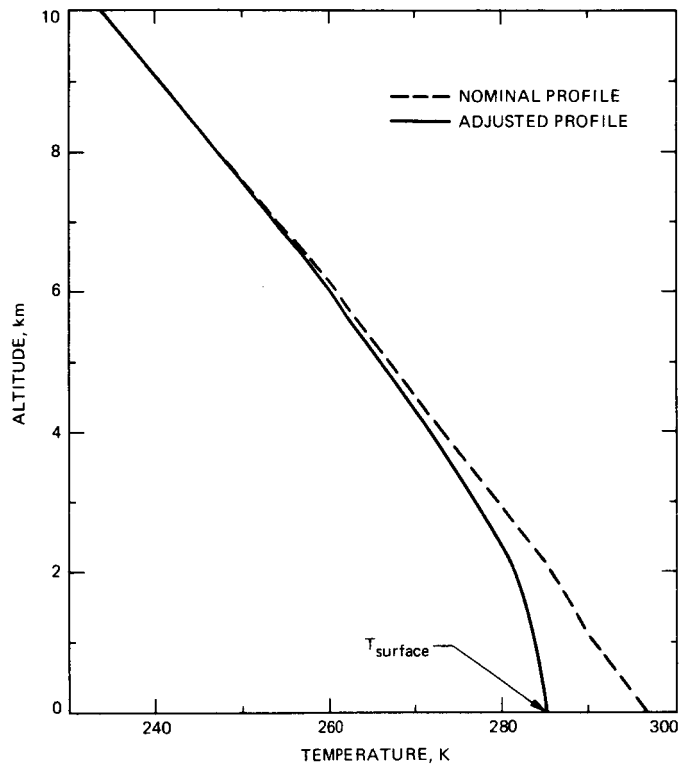


**Fig. 2.** An example of a nominal temperature profile derived from data in the Standard Atmosphere is represented by the dashed line. The solid line shows the temperature profile after it has been forced to match the measured surface temperature.